World Journal of Gastroenterology

Submit a Manuscript: http://www.wjgnet.com/esps/
Help Desk: http://www.wjgnet.com/esps/helpdesk.aspx
DOI: 10.3748/wjg.v20.i47.17839

World J Gastroenterol 2014 December 21; 20(47): 17839-17850
ISSN 1007-9327 (print) ISSN 2219-2840 (online)

ORIGINAL ARTICLE

Elevated free cholesterol in a p62 overexpression model of non-alcoholic steatohepatitis

Yvette Simon, Sonja M Kessler, Katja Gemperlein, Rainer M Bohle, Rolf Müller, Johannes Haybaeck, Alexandra K Kiemer

Yvette Simon, Sonja M Kessler, Alexandra K Kiemer, Department of Pharmacy, Pharmaceutical Biology, Saarland University, 66123 Saarbrücken, Germany
Sonja M Kessler, Johannes Haybaeck, Medical University of Graz, Institute of Pathology, Graz 8036, Austria
Katja Gemperlein, Rolf Müller, Department of Pharmacy, Pharmaceutical Biotechnology, Saarland University and Helmholtz Institute for Pharmaceutical Research Saarland (HIPS), Helmholtz Centre for Infection Research (HZI), 66123 Saarbrücken, Germany
Rainer M Bohle, Saarland University, Department of Pathology, 66421 Homburg, Germany
Author contributions: Simon Y and Kessler SM contributed equally to this paper; Simon Y, Kessler SM, Haybaeck J and Kiemer AK designed the experiments, analyzed the data and wrote the manuscript; Kiemer AK initiated and directed the study; Kessler SM, Bohle RM and Haybaeck J scored the histological slides; Gemperlein K and Müller R performed GC-MS lipid analyses; all authors had full access to all of the data (including statistical reports and tables) in the study and take responsibility for the integrity of the data and the accuracy of the data analysis.
Supported by An EASL Sheila Sherlock fellowship and a Bank Austria visiting scientist program fellowship (to Kessler SM)
Correspondence to: Alexandra K Kiemer, PhD, Department of Pharmacy, Pharmaceutical Biology, Saarland University, Campus C2 2, 66123 Saarbrücken,
Germany. pharm.bio.kiemer@mx.uni-saarland.de
Telephone: +49-681-30257301 Fax: +49-681-30257302
Received: April 11, 2014 Revised: June 15, 2014
Accepted: July 11, 2014
Published online: December 21, 2014

Abstract

AIM: To characterize how insulin-like growth factor 2 (*IGF2*) mRNA binding protein p62/IMP2-2 promotes steatohepatitis in the absence of dietary cholesterol.

METHODS: Non-alcoholic steatohepatitis (NASH) was induced in wild-type mice and in mice overexpressing p62 specifically in the liver by feeding the mice a methionine and choline deficient (MCD) diet for either two or four weeks. As a control, animals were fed a methionine and choline supplemented diet. Serum triglycerides, cholesterol, glucose, aspartate aminotransferase and alanine transaminase were determined by standard analytical techniques. Hepatic gene expression was determined by real-time reverse transcription-polymerase chain reaction. Generation of reactive oxygen species in liver tissue was quantified as thiobarbituric acid reactive substances using a photometric assay and malondialdehyde as a standard. Tissue fatty acid profiles and cholesterol levels were analyzed by gas chromatography-mass spectrometry after hydrolysis. Hepatocellular iron accumulation was determined by Prussian blue staining in paraffin-embedded formalin-fixed tissue. Filipin staining on frozen liver tissue was used to quantify hepatic free cholesterol levels. Additionally, nuclear localization of the nuclear factor kappa B (NF-κB) subunit p65 was examined in frozen tissues.

RESULTS: Liver-specific overexpression of the insulin-like growth factor 2 mRNA binding protein 2-2 (IGF2BP2-2/IMP2-2/p62) induces steatosis with regular chow and amplifies NASH-induced fibrosis in the MCD mouse model. Activation of NF-κB and expression of NF-κB target genes suggested an increased inflammatory response in *p62* transgenic animals. Analysis of hepatic lipid composition revealed an elevation of monounsaturated fatty acids as well as increased hepatic cholesterol. Moreover, serum cholesterol was significantly elevated in *p62* transgenic mice. Dietary cholesterol represents a critical factor for the development of NASH from hepatic steatosis. Filipin staining revealed increased free cholesterol in *p62* transgenic livers, which were not diet-derived. The mRNA levels of the rate-limiting enzyme for cholesterol synthesis 3-hydroxy-3-methyl-glutaryl-CoA reductase (HMG-CoA reductase or HMGCR) were not significantly upregulated, potentially due to increased cholesterol biosynthesis *via* elevated sterol regulatory element binding transcription factor 2 (*SREBF2*) gene expression and increased iron

deposition in transgenic animals.

CONCLUSION: This study provides evidence that p62/IGF2BP2-2 drives the progression of NASH through elevation of hepatic iron deposition and increased production of hepatic free cholesterol.

Key words: Insulin-like growth factor 2 mRNA binding protein 2-2; Methionine/choline deficient; Non-alcoholic fatty liver disease; Filipin; Iron

Core tip: Dietary cholesterol represents a critical factor for the development of non-alcoholic steatohepatitis (NASH) from steatosis. Liver-specific overexpression of the insulin-like growth factor 2 mRNA binding protein p62/IMP2-2/IGF2BP2-2 induces steatosis and amplifies NASH-induced fibrosis. Here, we show that p62 elevates monounsaturated fatty acids and hepatic cholesterol in the absence of exogenous cholesterol. Filipin staining demonstrates increased free cholesterol in *p62* transgenic livers. Srebf2-induced cholesterol biosynthesis in transgenics is most likely due to pronounced hepatic iron accumulation, which is also associated with lipid peroxidation in transgenic livers. In summary, p62/IGF2BP2-2 drives the progression of NASH by increasing hepatic free cholesterol.

Simon Y, Kessler SM, Gemperlein K, Bohle RM, Müller R, Haybaeck J, Kiemer AK. Elevated free cholesterol in a p62 overexpression model of non-alcoholic steatohepatitis. *World J Gastroenterol* 2014; 20(47): 17839-17850 Available from: URL: http://www.wjgnet.com/1007-9327/full/v20/i47/17839.htm DOI: http://dx.doi.org/10.3748/wjg.v20.i47.17839

INTRODUCTION

In industrialized countries, non-alcoholic fatty liver disease (NAFLD) represents the most frequent hepatic manifestation of chronic liver diseases, whereby hepatic steatosis is the first hit sensitizing the liver to a second hit that ultimately leads to hepatocyte injury, inflammation, and subsequent fibrotic changes[1]. Prolonged NAFLD can lead to hepatocellular carcinoma (HCC)[1], which is the sixth most common malignancy worldwide and the second leading cause of cancer-related deaths[2]. However, the pathophysiological mechanisms leading to the progression from NAFLD to end stage liver disease are still poorly understood.

The composition of fatty acids in the liver has emerged as a critical factor promoting the development of non-alcoholic steatohepatitis (NASH) and potentially HCC[3-7], with monounsaturated fatty acids (MUFA) implicated in a pathophysiological role[6,8]. Recent observations also highlighted the accumulation of free cholesterol as an important trigger for the progression from simple steatosis to severe NASH[9-11]. In fact, dietary cholesterol was demonstrated to be a critical factor in the progression of NASH[10,12]. Cholesterol fed to LDLR$^{-/-}$ mice induced a prominent inflammatory response, whereas high fat feeding without cholesterol induced steatosis in the absence of inflammation[13].

The insulin-like growth factor (IGF) 2 mRNA binding protein p62/IMP2-2/insulin-like growth factor 2 mRNA binding protein 2-2 (IGF2BP2-2) is a splice variant of IMP2/IGF2BP2 and was originally described as an autoantigen in an HCC patient[14]. p62 is upregulated in human HCC and its expression is correlated with poor prognosis[15,16]. Only physiological roles have been described for IMP2, which is required for proper nerve cell migration and morphology during development by controlling cytoskeletal remodeling and dynamics (reviewed in[17]). We recently reported that mice with liver-specific overexpression of p62 develop a fatty liver and show increased development towards NASH-induced fibrosis[4,18,19]. This amplification of an inflammatory response was observed in a feeding model that omitted dietary cholesterol. We therefore aimed to investigate the mechanisms involved in the amplification of NASH by p62 in the absence of dietary cholesterol.

A methionine/choline deficient (MCD) diet without supplementation of cholesterol was fed to *p62* transgenic animals. The MCD diet is the most commonly used murine dietary model for acquired NASH, since in contrast to other models, it allows examination of all stages of NASH (*i.e.*, inflammation, oxidative stress, and fibrogenic changes)[20].

Our data implicate p62 as a modulator of endogenous cholesterol synthesis leading to elevated levels of free cholesterol in the liver, ultimately promoting inflammation *via* the activation of nuclear factor kappa B (NF-κB). Moreover, the elevated levels of hepatocellular iron link lipid metabolism to the promotion of inflammatory reactions[21].

MATERIALS AND METHODS

Material

The MCD diet (#960439) and the methionine/choline supplemented control (ctrl) diet (#960441), both containing 45% sucrose and 10% corn oil without cholesterol, were purchased from MP Biomedicals (Heidelberg, Germany). Polymerase chain reaction (PCR) primers were obtained from Eurofins MWG Operon (Ebersberg, Germany). The EvaGreen® qPCR Mix was obtained from Solis BioDyne (Tartu, Estonia). Antibodies and immunofluorescence conditions are detailed in Table 1.

Animal treatment

All animal procedures were performed under the guidelines of the local animal welfare committee (permission No. 34/2010). Mice were kept on a 12-h dark-light cycle under controlled conditions (temperature: 22 ℃ ± 2 ℃; relative humidity: 55% ± 10%) with unrestricted access to food and water until the age of three weeks.

Mice were randomly divided into experimental groups

Table 1 Antibody dilution, unmasking, incubation time, temperature, and immunodetection used for immunofluorescence

Antibody (source)	Unmasking of antigens	Dilution	Incubation	Detection system
NF-κB p65 (Neomarkers, United States)	Citrate buffer pH 6.0, 95 ℃, 10 min, water bath	1:1000	18 h at 4 ℃	IF with Alexa Fluor 546 (Invitrogen, Germany) as secondary antibody

NF-κB: Nuclear factor kappa B; IF: Immunofluorescence.

Table 2 Primer sequences for real-time reverse transcription-polymerase chain reaction

mRNA	Accession No.	Sense primer, 5'→3'	Antisense primer, 5'→3'
18S	NR_003278.1	GTAACCCGTTGAACCCCATT	CCATCCAATCGGTAGTAGCG
PPARa	NM_001113418.1	CCTTCCCTGTGAACTGACG	CCACAGAGCGCTAAGCTGT
IL-1B	NM_008361.3	GAGAGCCTGTGTTTTCCTCC	GAGTGCTGCCTAATGTCCC
TNF	NM_013693.2	CCATTCCTGAGTTCTGCAAAGG	AGGTAGGAAGGCCTGAGATCTTATC
HMGCR	NM_008255.2	ATCCAGGAGCGAACCAAGAGAG	CAGAAGCCCCAAGCACAAAC
SCD1	NM_009127.4	AGATCTCCAGTTCTTACACGACCAC	CTTTCATTTCAGGACGGATGTCT
CPT1a	NM_013495.2	CTCAGTGGGAGCGACTCTTCA	GGCCTCTGTGGTACACGACAA
NOS2	NM_010927.3	CTCACTGGGACAGCACAGAA	GATGTGGCCTTGTGGTGAA
PTGS/COX2	XM_192868	TGACCCCCAAGGCTCAAATAT	TGAACCCAGGTCCTCGCTTA
FASN	NM_007988.3	GGCTGCTACAAACAGACCAT	CACGGTAGAAAAGGCTCAGT
SREBF2	NM_033218.1	ACCTAGACCTCGCCAAAGGT	CGGATCACATTCCAGGAGA

PPARa: Peroxisome proliferator-activated receptor a; IL-1B: Interleukin 1B; TNF: Tumor necrosis factor; HMGCR: 3-hydroxy-3-methyl-glutaryl-CoA reductase; SCD1: Stearoyl-CoA desaturase 1; CPT1a: Carnitine palmitoyl transferase 1a; NOS2: Nitric oxide synthase 2; PTGS/COX2: Prostaglandin-endoperoxide synthase 2; FASN: Fatty acid synthase; SREBF2: Sterol regulatory element binding transcription factor 2.

Table 3 Scoring system for hepatocellular iron and nuclear factor kappa B-p65 nuclear translocation

Scoring system		Assessed by
Hepatocellular iron		
Score 0	No granules	Prussian blue
Score 1	Zone 1, granules seen at × 40	
Score 2	Granules seen at × 20	
Score 3	Granules seen at × 10	
Score 4	Granules seen at × 10 in zone 1 and 2	

NF-κB: Nuclear factor kappa B; IF: Immunofluorescence.

at the age of 3 wk and fed an MCD diet or an MCD diet supplemented with choline bitartrate (2 g/kg) and DL-methionine (3 g/kg) for two or four weeks; the latter was designated as the ctrl diet[18]. Male and female wild-type or *p62* transgenic mice were used as previously described[19].

Serum parameters

Animals were sacrificed and serum levels were determined at the Zentrallabor des Universitätsklinikums des Saarlandes (Homburg, Germany).

Real-time reverse transcription-polymerase chain reaction

Experiments and quantification were performed as previously described[22]. Primer sequences are listed in Table 2.

Quantification of thiobarbituric acid reactive substances

Products of lipid peroxidation were measured by a fluorimetric assay. Liver tissues (10-20 mg) were homogenized in PBS (Na_2HPO_4 8.0 mmol/L, KH_2PO_4 1.5 mmol/L, NaCl 160 mmol/L in water) containing 1% phosphatase inhibitor cocktail Ⅱ (Sigma-Aldrich, Taufkirchen, Germany), and centrifuged. For protein precipitation, 100 μL lysate was mixed with 200 μL ice cold 10% trichloroacetic acid and after incubation on ice, centrifuged for 10 min at 14000 *g*. The clear supernatant was mixed with an equal volume of thiobarbituric acid (TBA) [0.67% (w/v)], and heated for 15 min at 100 ℃. After cooling the supernatant down to room temperature, the fluorescence intensity of the samples was measured in duplicate in a 96 well plate at $\lambda_{ex/em}$ = 530 nm/572 nm. Thiobarbituric acid reactive substances (TBARS) are expressed as malondialdehyde (MDA) equivalents as μmol per mg liver tissue. An MDA standard was used to create a standard curve, against which unknown samples were plotted.

Fatty acid profile analysis

Snap-frozen liver tissue samples were lyophilized until dry (approximately 10 mg dry weight). Fatty acid extraction and alkaline hydrolysis was performed using the fatty acid methyl ester method and measured with GC-MS as previously published[3,23].

Histology and immunohistochemistry

For histological examination, paraffin-embedded liver tissue specimens were cut and stained with Prussian blue to evaluate iron accumulation. Immunofluorescent staining was performed after unmasking of the sections (Table 1). The sections were immunostained with the appropriate antibody; concentration and incubation time and temperature are listed in Table 1. Staining for unesterified "free" cholesterol was performed on frozen liver sections with filipin, which identifies free cholesterol[11]. Quantification was performed with Image J software on five randomly

Table 4 Liver weight and serum parameters of *p62* transgenic and wild-type mice fed a methionine-choline deficient diet or control diet for two and four weeks

	2 wk				4 wk			
	ctrl		MCD		ctrl		MCD	
	wt	tg	wt	tg	wt	tg	wt	tg
Number of animals	10	10	12	12	10	10	12	12
Relative liver weight (% of body weight)	4.8 ± 0.1	4.6 ± 0.1	3.4 ± 0.1[c]	4.0 ± 0.2[a,c,e]	4.2 ± 01	4.1 ± 0.1	3.4 ± 0.1[c]	3.5 ± 0.2[c,e]
Serum ALT (U/L)	289 ± 83	233 ± 20	418 ± 36[c]	469 ± 73[c,e]	189 ± 38	222 ± 25	235 ± 40	209 ± 46
Serum AST (U/L)	1568 ± 224	1535 ± 162	2404 ± 125[c]	2544 ± 207[c,e]	1845 ± 204	1712 ± 253	2813 ± 286[c]	3057 ± 346[c]
Serum triglycerides (mg/dL)	244 ± 19	219 ± 17	107 ± 5[c]	128 ± 11[c,e]	211 ± 18	203 ± 21	95 ± 7[c]	106 ± 5[c,e]
Serum HDL (mg/dL)	94 ± 6	98 ± 4	24 ± 2[c]	21 ± 4[c,e]	112 ± 8	119 ± 8	15 ± 2[c]	18 ± 2[c,e]
Serum glucose (mg/dL)	234 ± 27	179 ± 15	67 ± 10[c]	59 ± 7[c,e]	193 ± 13	253 ± 36	59 ± 7[c]	40 ± 5[a,c,e]

[a]$P < 0.05$ *vs* wild-type; [c]$P < 0.05$ *vs* control diet; [e]$P < 0.05$ *vs* wild-type on control diet; Values are expressed as the mean ± SEM; tg: Transgenic; wt: Wild-type; ctrl: Control; MCD: Methionine-choline deficient.

selected pictures from each sample. NF-κB-p65 staining was performed as previously published[24]. Counterstaining with either Nuclear fastred for histochemistry or 4',6'-diamidine-2-phenylindol (DAPI) for immunofluorescence (IF) was performed and sections were dehydrated and embedded with Entellan® (#107961, Merck, Germany). As a negative control, sections were incubated without primary antibody.

Three investigators, blinded to all experimental conditions (SMK, RMB, JH), examined the sections for hepatocellular iron and NF-κB-p65 nuclear translocation (Table 3).

Statistical analysis

Data analysis and statistics were performed using Microsoft Office 2010 and OriginPro 8.6 G. The effect of genotype, MCD diet, and their interactions were displayed as mean values ± SEM with 10-12 animals per group. Statistical differences were estimated using the Kruskal-Wallis-ANOVA for nonparametric samples followed by post-hoc-analysis with the Mann-Whitney *U* test. Differences were considered statistically significant when *P* values were less than 0.05.

RESULTS

General effects of dietary manipulation

Mice of both genotypes exhibited different characteristics typical of the MCD diet. Specifically, we observed a loss of body mass and relative liver weight through feeding the MCD diet (Table 4). Due to reduced very low density lipoprotein (VLDL) secretion from the liver[25], serum triglycerides and cholesterol were reduced in MCD animals, as were serum glucose levels. *p62* transgenic animals exhibited a further reduction in serum glucose levels as previously reported[18], most likely due to elevated IGF2 production. Elevated aspartate aminotransferase (AST) and alanine transaminase (ALT) levels indicated liver damage induced by the MCD diet, as previously described[26] (Table 4).

p62 amplifies inflammation

Since p62 promotes NASH-induced fibrosis paralleled by increased expression of the chemokine monocyte chemoattractant protein 1 (MCP1)/chemokine ligand 2 (CCl2)[18], our previous data suggested that p62 elicits an increased inflammatory response during NASH. Histological detection of activated NF-κB was assessed by nuclear translocation of its subunit *p65*, and suggested an elevated immune response in *p62* transgenics (Figure 1A). This elevated response was confirmed by an NF-κB-dependent gene expression profile, which showed increased levels of tumor necrosis factor (*TNF*) (Figure 1B), inducible nitric oxide synthase 2 (*Nos2*) (Figure 1C), prostaglandin-endoperoxide synthase 2 (*PTGS/COX2*) (Figure 1D), and interleukin (*IL*) 1B in *p62* transgenic mice (Figure 1E).

p62 alters the fatty acid pattern

Animals of both genotypes developed steatosis on the MCD diet. However, previous histological analyses suggested an amplification of steatosis in *p62* transgenic animals compared to their wild-type littermates[18]. After two weeks, the relative liver weight was significantly increased in transgenics ($P = 0.02$) (Table 4) and therefore consistent with the histological changes. GC-MS analyses revealed significantly higher levels of hepatic fatty acids in *p62* transgenic mice (Figure 2A), whereas serum triglycerides were unchanged (Table 4). The hepatic fatty acid pattern indicated strong alterations in *p62* transgenic animals compared to their wild-type littermates after two weeks on the MCD diet (Table 5). In particular, a more pronounced accumulation of MUFA compared to saturated fatty acids (SFA) and polyunsaturated fatty acids (PUFA) was observed in transgenic animals (MUFA: 68% increase *vs* SFA: 40% and PUFA: 45%) (Figure 2B). Both the distinct elevation of palmitoleic acid (C16:1) and oleic acid (C18:1) (Figure 2C) indicated increased desaturase activity. Gene expression of the desaturase stearoyl-CoA desaturase (*SCD*) 1, which is responsible for the formation of C16:1 and C18:1 fatty acids, tended to be increased in *p62* transgenic animals, despite a strong downregula-

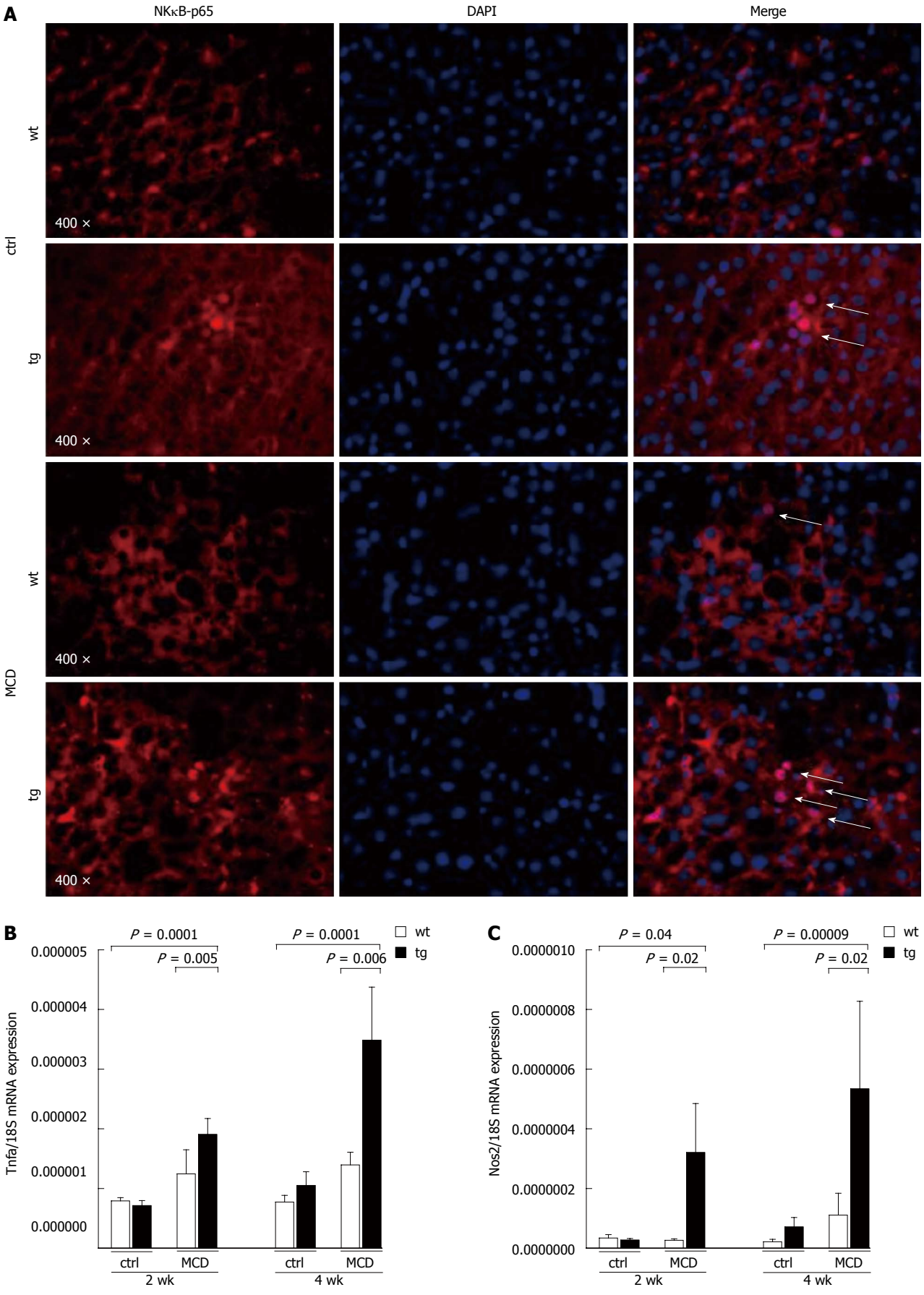
A
NKκB-p65
DAPI
Merge
ctrl
wt
tg
MCD
wt
tg
400 ×
400 ×
400 ×
400 ×
B
P = 0.0001
P = 0.005
P = 0.0001
P = 0.006
wt
tg
Tnfa/18S mRNA expression
0.000005
0.000004
0.000003
0.000002
0.000001
0.000000
ctrl
MCD
ctrl
MCD
2 wk
4 wk
C
P = 0.04
P = 0.02
P = 0.00009
P = 0.02
wt
tg
Nos2/18S mRNA expression
0.0000010
0.0000008
0.0000006
0.0000004
0.0000002
0.0000000
ctrl
MCD
ctrl
MCD
2 wk
4 wk

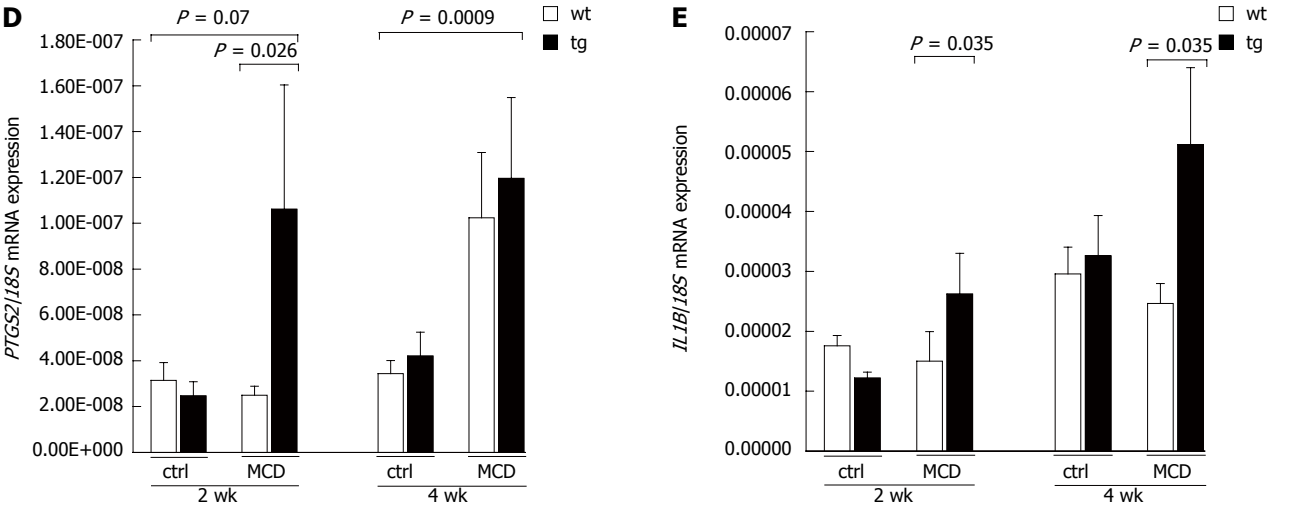

Figure 1 p62 expression amplifies inflammation. A: Immunofluorescent staining with anti-nuclear factor kappa B (NF-κB)-p65 (red, left panel), 4',6-diamidino-2-phenylindole (DAPI) for nuclei (blue, middle panel), and merge (right panel) shows activation of NF-κB after four weeks on the methionine-choline deficient (MCD) diet through *p65* translocation to the nucleus (white arrows) (original magnification: × 400); B-E: Gene expression analysis from quantitative real-time reverse transcription-polymerase chain reaction (RT-PCR) of NF-κB target genes with tumor necrosis factor (TNF) (B), inducible nitric oxide synthase 2 (*NOS2*) (C), prostaglandin-endoperoxide synthase 2 (*PTGS/COX2*) (D), and interleukin 1B (*IL-1B*) (E) from whole livers are expressed as a ratio against the housekeeping gene, *18S*. Data are presented as the mean ± SEM (*n* = 10-12). ctrl: Control; wt: Wild type; tg: Transgenie.

tion on the MCD diet (Figure 2D). Expression of other lipogenic and fatty acid catabolism regulators, such as the fatty acid synthase (*FASN*), the lipolysis regulator peroxisome proliferator-activated receptor a (*PPARa*), and the promotor of β-oxidation, carnitine palmitoyl transferase 1a (*CPT1a*), were not altered upon *p62* expression when mice were fed the MCD diet (Figure 2D).

Elevated cholesterol in p62 transgenic animals

Both liver cholesterol as well as serum cholesterol were distinctly elevated in *p62* transgenic mice (Figure 3A and B). Filipin staining for free cholesterol revealed a significant increase in free cholesterol in *p62* transgenic animals on the MCD diet (Figure 3C, D). While the mRNA levels of *HMGCR* were not significantly upregulated (Figure 3E), the expression of the cholesterol metabolism-related transcription factor sterol regulatory element binding transcription factor 2 (*SREBF2*) was significantly increased after four weeks (Figure 3F).

p62 induces hepatocellular iron deposition and lipid peroxidation

Because cholesterol biosynthesis was previously reported to be induced by elevated hepatic iron[27], iron deposition was next evaluated. Both genotypes on the MCD diet had elevated hepatic iron deposition with a more distinct iron accumulation in *p62* transgenic mice (Figure 4A, B). Interestingly, iron deposition was also detected in transgenic, but not in wild-type mice on the ctrl diet (Figure 4B). Since hepatocellular iron is a promoter of oxidative stress, we assessed lipid peroxidation. Accordingly, p62 expression significantly increased lipid peroxidation as analyzed by a TBARS assay on the control diet at two weeks and, on the MCD diet, a respective trend was observed at four weeks (Figure 4C).

DISCUSSION

The fatty acid composition and the accumulation of free cholesterol have been implicated in playing a critical role in the development of NASH since an altered lipidome[3,11,12] as well as free cholesterol, positively correlate with the severity of NASH[10,12,28,29]. Dietary cholesterol may play a role in NAFLD onset[30]. In the current study, we describe an increased production of free cholesterol in mice with liver-specific overexpression of p62 in the absence of dietary cholesterol.

Because elevated activation of NF-κB is observed in *p62* transgenic animals, they are more prone to an inflammatory response in this model of NASH. Accordingly, gene expression of inflammatory mediators such as TNF were elevated in these animals, which has previously been shown for MCP1/CCl2[18]. TNF is strongly correlated with fatty acid metabolism as it negatively regulates the expression of PPARa, leading to decreased catabolism[31]. In human NAFLD, elevated serum TNF levels in patients are a strong indicator for the progression from steatosis to NASH[32].

Surprisingly, we detected a lower apoptosis rate in *p62* transgenic mice when we examined cleaved caspase-3 by immunohistochemistry, counteracting the apoptosis-inducing effect of TNF[33]. Additionally, *p62* transgenic animals did not show an induction of liver damage despite elevated fat and inflammation, which is in contrast to elevated AST and ALT levels in human NASH[34]. The combination of less apoptosis and liver damage confirms the cytoprotective properties of p62[16,19] and may highlight a correlation with the cytoprotective actions of MUFAs[6]. The increase of *IL-1B* mRNA as a result of NF-κB activation in *p62* transgenic animals might further link early lipidomic changes in steatosis with progression to a

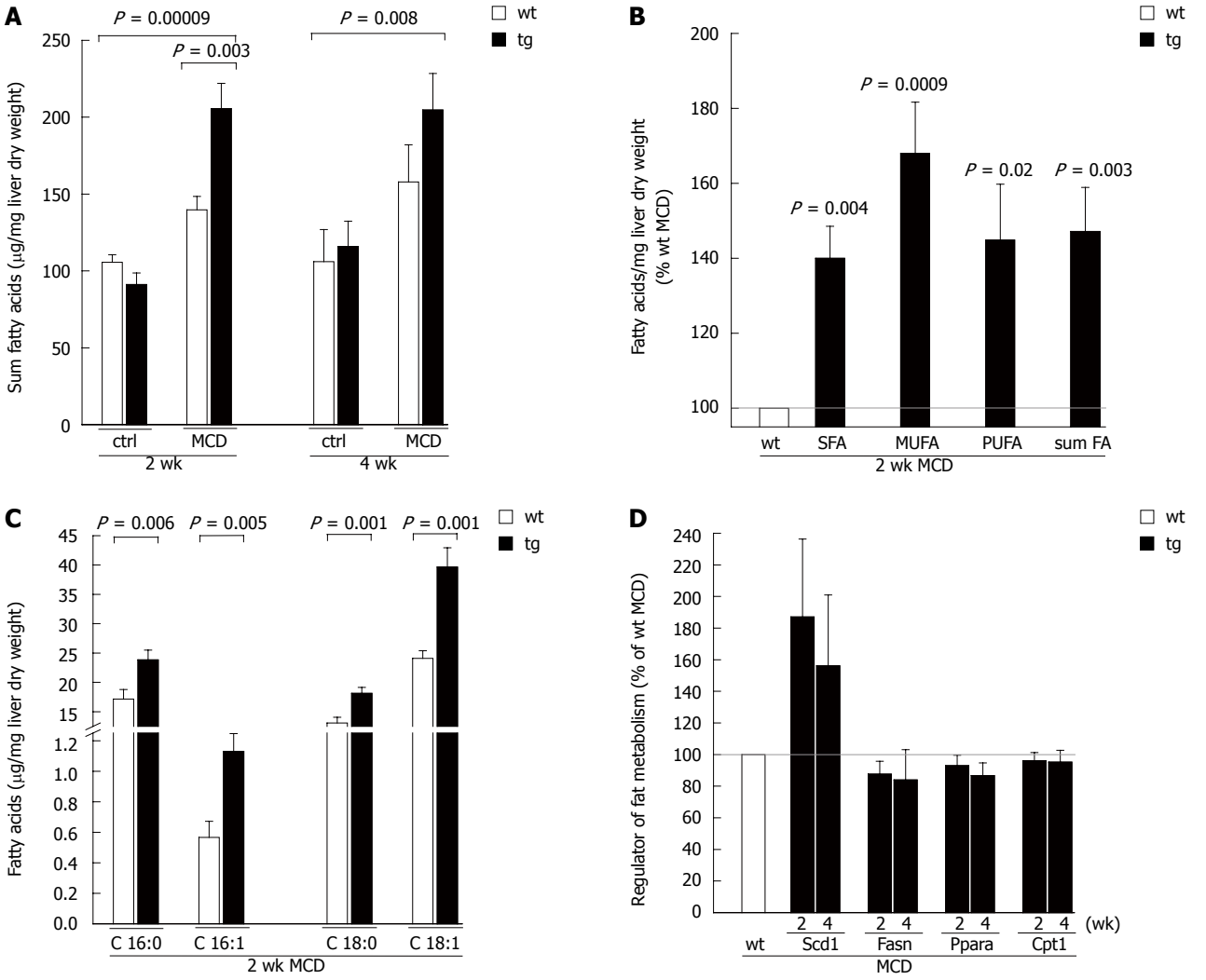

Figure 2 p62 alters the fatty acid pattern. A: Sum of all fatty acids in mice fed the methionine-choline deficient (MCD) or ctrl diet for two and four weeks. Liver tissues were lyophilized, lipids were hydrolyzed, and fatty acids (FA) were analyzed by gas-chromatography mass-spectrometry (GC-MS); B: Sum of the saturated fatty acids (SFA), monounsaturated fatty acids (MUFA), polyunsaturated fatty acids (PUFA), and all fatty acids (sum FA) from animals fed the MCD diet for two weeks are presented as the mean ± SEM (n = 9-12). Data are displayed as the percentage of MCD-fed wild-type mice, which were set to 100%, each; C: Palmitic acid (C16:0), palmitoleic acid (C16:1), stearic acid (C18:0), and oleic acid (C18:1) are presented as the mean ± SEM (n = 9-12); D: Relative hepatic mRNA expression of stearoyl-CoA desaturase (SCD) 1, fatty acid synthase (FASN), peroxisome proliferator-activated receptor a (PPARa), and carnitine palmitoyl transferase (CPT) 1a from mice fed the MCD diet for two and four weeks were normalized against the housekeeping gene *18S* and are shown as the percentage of MCD-fed wild-type mice, which were set to 100%, each. Data are presented as the mean ± SEM (n = 10-12). tg: Transgenic; wt: Wild-type; ctrl: Control.

strong inflammatory response[35,36].

Interestingly, the amount of MUFA was increased relative to SFA and PUFA in *p62* transgenic animals, indicating that there are alterations in the fatty acid metabolism in both NASH and NASH-related HCC[3,6]. Increased MUFAs are correlated with hypertriglyceridemia and obesity[37], without exogenous ingestion, due to hepatic synthesis. In animal studies, exogenous MUFAs were found to be protective against MCD-induced NASH[8].

Desaturases represent the rate-limiting enzymes for the production of palmitoleic (C16:1) and oleic acid (C18:1), with SCD1 being the predominant form in the liver[38,39]. In this study, we observed an increase in SCD1 in *p62* transgenic animals, despite a strong downregulation on the MCD diet. In human NASH-related HCC tissues, an upregulation of SCD1 was also found[6]. The expression of FASN was found to be downregulated with the MCD diet without differences among the genotypes, similar to other murine models of steatohepatitis[31,40] and human NASH[28]. We also found no changes for the lipolysis regulators PPARa and CPT1 in *p62* transgenic mice.

p62 transgenic mice fed the MCD diet showed hyperlipidemia with increased serum cholesterol levels. These findings are particularly interesting given that the MCD diet is known for lowered serum triglyceride (TG) levels and, in this particular case, differs from human NASH[41]. To our knowledge, this is the first time that an increase in hepatic total and free cholesterol has been documented in a nutritional mouse model without exogenous cholesterol. Increased dietary cholesterol intake is associated with risk and severity of NAFLD and is paralleled by hepatic free cholesterol accumulation in human as well as in experimental settings[42] and even differentiates steatosis from

Table 5 Gas-chromatography mass-spectrometry fatty acid analyses of mice fed the methionine-choline deficient or control diet for two weeks

Fatty acid	ctrl wt	ctrl tg	*P* value[1]	MCD wt	MCD tg	*P* value[2]	*P* value[3]
14:0	0.25 ± 0.04	0.25 ± 0.05	0.970	0.24 ± 0.04	0.43 ± 0.04	0.003	0.005
15:0	0.01 ± 0.003	0.01 ± 0.003	0.113	0.02 ± 0.01	0.05 ± 0.01	0.035	0.002
16:0	17.23 ± 0.79	16.08 ± 1.43	0.623	17.16 ± 1.63	23.85 ± 1.65	0.006	0.0033
16:1	1.69 ± 0.29	1.51 ± 0.30	0.570	0.57 ± 0.10	1.13 ± 0.12	0.005	0.138
17:0	0.11 ± 0.01	0.06 ± 0.01	0.021	0.23 ± 0.03	0.34 ± 0.03	0.010	0.0001
17:1	0.02 ± 0.01	0.01 ± 0.01	0.046	0.003 ± 0.003	0.01 ± 0.01	0.514	0.117
18:0	12.64 ± 0.57	9.41 ± 0.81	0.006	13.08 ± 0.97	18.15 ± 1.00	0.0014	0.0009
18:1	20.13 ± 2.51	17.98 ± 2.07	0.678	24.11 ± 1.28	39.66 ± 3.27	0.001	0.0009
18:2	17.88 ± 0.87	16.42 ± 1.60	0.241	23.90 ± 2.15	36.28 ± 6.34	0.040	0.004
18:3	0.23 ± 0.05	0.27 ± 0.10	0.571	1.50 ± 0.28	2.99 ± 0.46	0.003	0.00009
20:0	0.22 ± 0.05	0.10 ± 0.03	0.045	0.14 ± 0.03	0.33 ± 0.05	0.0007	0.138
20:1	0.40 ± 0.03	0.30 ± 0.04	0.045	0.81 ± 0.14	1.99 ± 0.27	0.002	0.00009
20:2	0.45 ± 0.04	0.53 ± 0.06	0.385	1.67 ± 0.17	2.94 ± 0.25	0.0006	0.00009
20:3	1.09 ± 0.09	0.89 ± 0.14	0.186	2.87 ± 0.37	5.15 ± 0.44	0.0006	0.00009
20:4	13.69 ± 0.58	10.37 ± 0.80	0.011	16.49 ± 1.15	23.20 ± 1.81	0.006	0.00015
22:0	0.59 ± 0.11	0.29 ± 0.07	0.031	0.31 ± 0.03	0.50 ± 0.03	0.0007	0.921
22:1	0.01 ± 0.003	0.003 ± 0.003	0.387	0.01 ± 0.01	0.04 ± 0.01	0.091	0.129
22:4	0.57 ± 0.05	0.51 ± 0.08	0.273	4.24 ± 0.48	6.25 ± 0.56	0.0036	0.00009
22:6	4.72 ± 0.28	3.82 ± 0.29	0.054	12.08 ± 0.90	14.06 ± 1.05	0.214	0.00009
23:0	0.08 ± 0.01	0.04 ± 0.004	0.0003	0.08 ± 0.01	0.10 ± 0.01	0.194	0.223
24:0	0.42 ± 0.02	0.31 ± 0.02	0.003	0.45 ± 0.02	0.63 ± 0.05	0.0013	0.0009

[1]*P* value of the comparison between ctrl wt and ctrl tg; [2]*P* value of the comparison between MCD wt and MCD tg; [3]*P* value of the comparison between ctrl wt and MCD tg; Values (μg/mg dry liver tissue) are expressed as the mean ± SEM. Liver tissues were lyophilized and analyzed by gas-chromatography mass-spectrometry. tg: Transgenic; wt: Wild-type; ctrl: Control; MCD: Methionine-choline deficient.

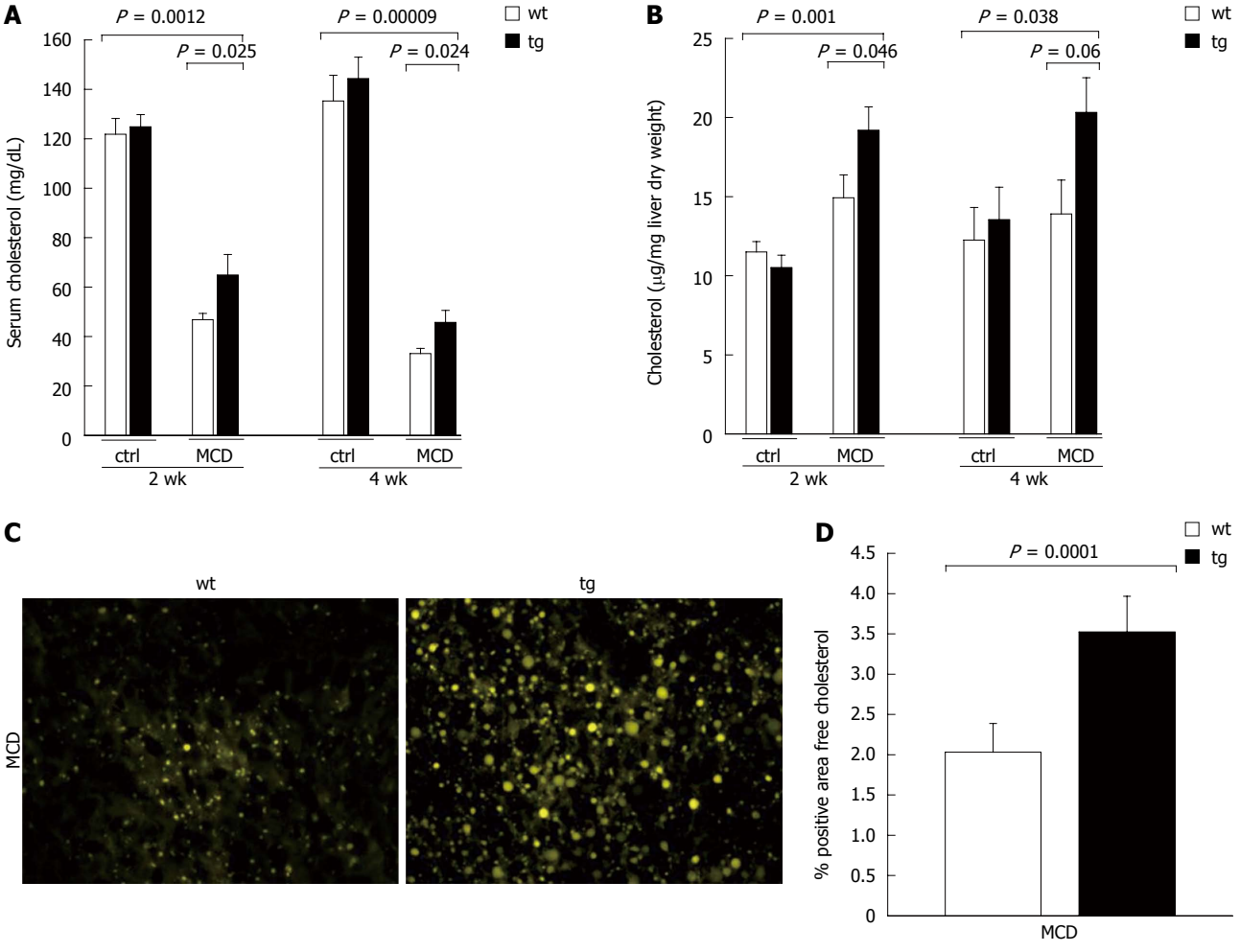

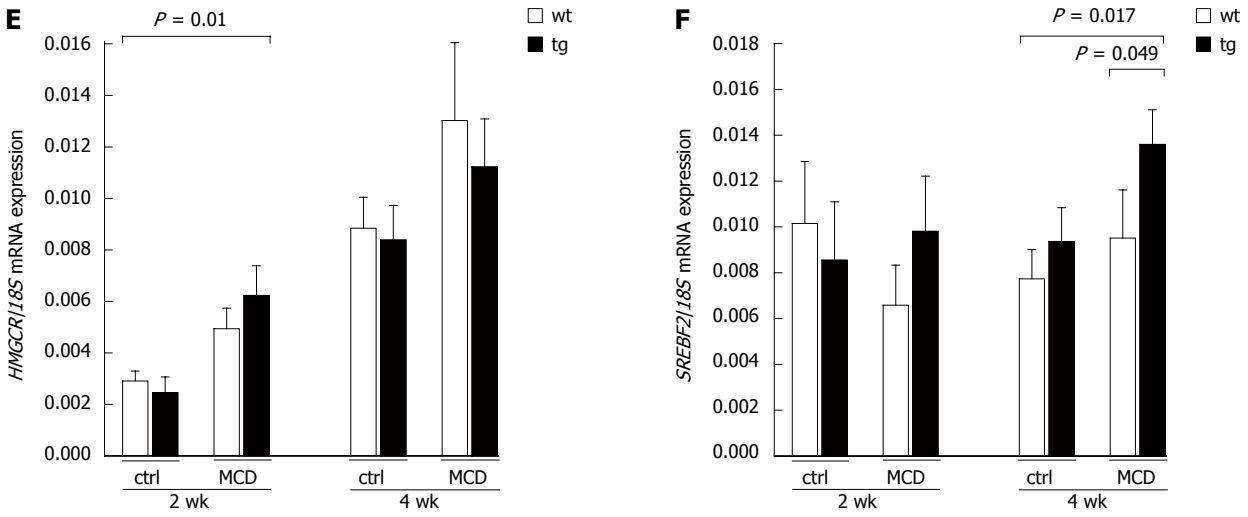

Figure 3 p62 expression elevates serum and liver cholesterol. A, B: Hepatic (A) and serum (B) cholesterol concentrations in mice fed the respective diet for two or four weeks; C, D: Representative cryosections stained with Filipin for hepatic free cholesterol in mice fed the methionine-choline deficient (MCD) diet for four weeks (original magnification: × 400) (C) with corresponding quantification (D) (mean out of five randomly picked sections on the slide); E, F: Relative hepatic mRNA expression of 3-hydroxy-3-methyl-glutaryl-CoA reductase (HMG-CoA reductase or *HMGCR*) (E) and sterol regulatory element binding transcription factor 2 (*SREBF2*) (F) are shown as a ratio against the housekeeping gene, *18S*. Data are presented as the mean ± SEM (n = 10-12). tg: Transgenic; wt: Wild-type; ctrl: Control.

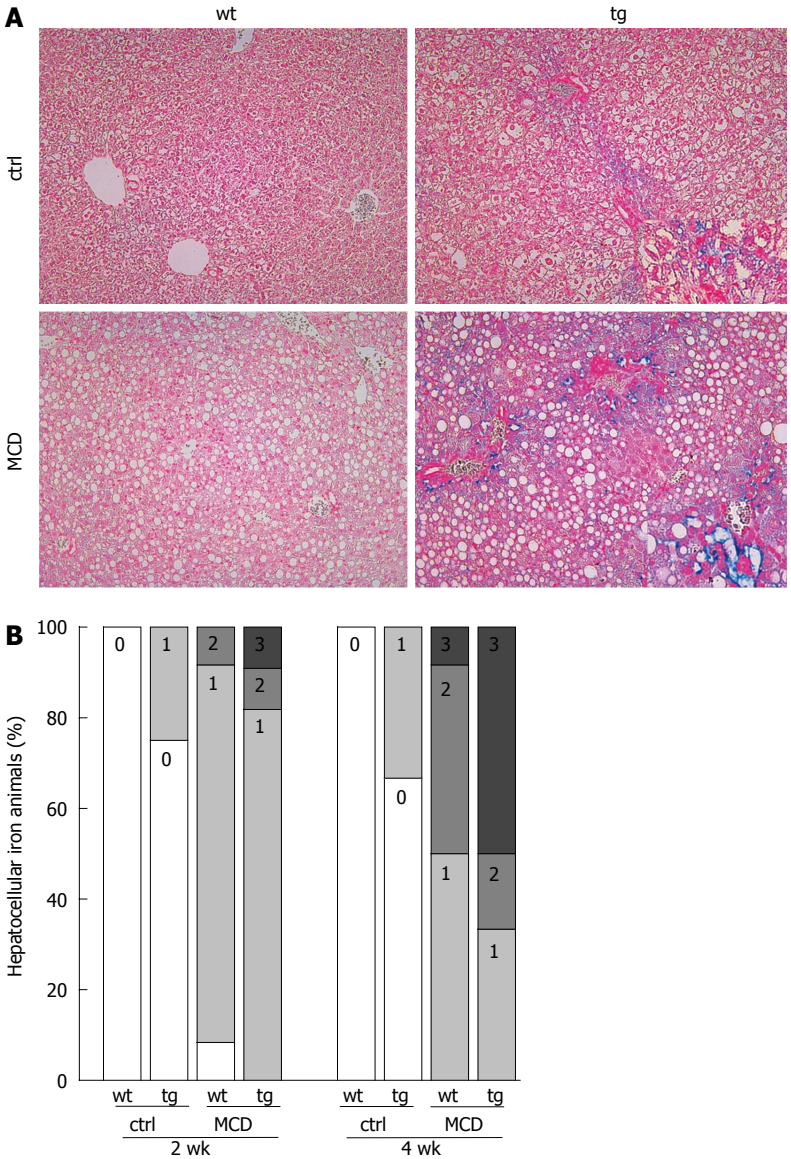

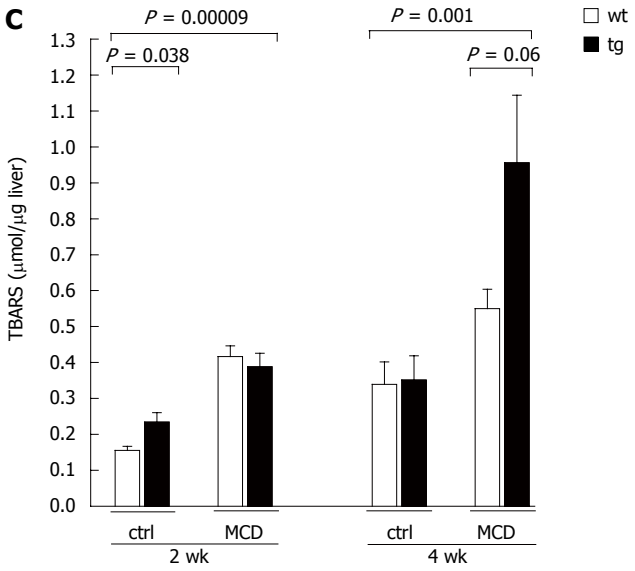

Figure 4 p62 expression leads to increased iron accumulation and reactive oxygen species production. A, B: Representative paraffin-embedded liver sections stained with Prussian blue for iron accumulation from animals fed the respective diet for four weeks (original magnification × 200 and × 500 for inserts) (A) with the corresponding hepatocellular iron score (B) for all time points (for scoring, see supplement S1); C: Hepatic thiobarbituric acid reactive substances (TBARS) were measured to indicate lipid peroxidation and are presented as the mean ± SEM (*n* = 10-12). tg: Transgenic; wt: Wild-type; ctrl: Control; MCD: Methionine and choline deficient.

NASH[43]. Besides dietary cholesterol intake, cellular cholesterol accumulation may result from disturbed cholesterol homeostasis[42]. Here, we observed enhanced expression of SREBF2, but no distinct effect on the expression of the rate-limiting enzyme HMGCR. While a positive correlation between the severity of NASH with the expression of these genes was found[29], others reported no correlation between SREBF2 and hepatic cholesterol despite elevated HMGCR[27]. Interestingly, however, cholesterol biosynthesis was found to be positively correlated with iron accumulation: when additional iron was given, it led to deposition of free cholesterol and an upregulation of cholesterol biosynthesis[27]. Furthermore, hepatocellular iron deposition was reported to be elevated in human NASH patients[44] and NASH-related HCC patients[45]. Variations in hepatic iron levels can directly lead to a modulation of lipogenesis and lipid storage and secretion, as iron is an integral part of several lipid metabolism related enzymes[46]. In this context, SCD1 activity has been shown to be iron-dependent, as the protein contains iron as a cofactor[47]. Accordingly, the iron accumulation in *p62* transgenic mice might elevate SCD1 activity.

Enhanced iron accumulation is also related to enhanced lipid peroxidation[44] since iron is known to catalyze the production of reactive oxygen species, which can then initiate cellular damage and lipid peroxidation[48]. In fact, reactive oxygen species have been suggested as critical contributors to the second hit required for disease onset[49]. Elevated production of reactive oxygen species in *p62* transgenics on the ctrl diet, which correlates with the iron accumulation in these animals, might predispose them towards the development of NASH.

Taken together, this study reveals that liver-specific overexpression of p62 leads to an amplified progression of NAFLD towards NASH through increased production of hepatic free cholesterol driving the inflammatory response in liver disease.

ACKNOWLEDGMENTS

We thank Eva Dilly for technical assistance in both animal care and experiments. We thank Christina Guth at the Leibniz Institute for New Materials (INM) for support in microscopy.

COMMENTS

Background

In industrialized countries, non-alcoholic fatty liver disease (NAFLD) represents the most frequent chronic liver disease and is a potential risk factor for the development of hepatocellular carcinoma (HCC), the most common primary liver cancer. HCC, an aggressive cancer with high mortality, is difficult to detect and treat. The insulin-like growth factor (IGF) 2 mRNA binding protein p62 was originally discovered in an HCC patient. p62 induces fatty liver and promotes non-alcoholic steatohepatitis (NASH)-induced fibrosis.

Research frontiers

Dietary cholesterol represents a critical factor in the development of NASH from hepatic steatosis. In this context, the accumulation of free cholesterol was recently highlighted as important trigger for the progression from simple steatosis to severe NASH. Recently, the role of free cholesterol and iron accumulation in NASH progression have been actively researched. Whether and how elevated free cholesterol can accumulate independently of dietary cholesterol is a current topic of strong interest.

Innovations and breakthroughs

The authors show for the first time that free cholesterol can accumulate and promote NAFLD in the absence of dietary cholesterol. The IGF2 mRNA binding protein p62 facilitates increased levels of both free cholesterol and hepatic iron. Furthermore, hepatic iron accumulation was associated with lipid peroxidation. In summary, this study shows that p62 drives the progression of NASH by increasing hepatic free cholesterol.

Applications

The understanding of how p62 promotes NASH progression and further characterization of the role of specific lipid changes will increase knowledge about

NASH pathogenesis and might therefore aid in the development of preventive strategies against NASH and NASH-associated HCC. This might also lead to new therapeutic options in NASH treatment.

Terminology

Free cholesterol: cholesterol not esterified with a fatty acid.

Peer review

The data show that p62/IGF2BP2-2 drives the progression of NASH by increasing hepatic free cholesterol. This study is well executed and relevant to clinicians and scientists studying NASH and NAFLD.

REFERENCES

1 **Cohen JC**, Horton JD, Hobbs HH. Human fatty liver disease: old questions and new insights. *Science* 2011; **332**: 1519-1523 [PMID: 21700865 DOI: 10.1126/science.1204265]

2 **El-Serag HB**. Hepatocellular carcinoma. *N Engl J Med* 2011; **365**: 1118-1127 [PMID: 21992124 DOI: 10.1056/NEJMra1001683]

3 **Kessler SM**, Simon Y, Gemperlein K, Gianmoena K, Cadenas C, Zimmer V, Pokorny J, Barghash A, Helms V, van Rooijen N, Bohle RM, Lammert F, Hengstler JG, Mueller R, Haybaeck J, Kiemer AK. Fatty acid elongation in non-alcoholic steatohepatitis and hepatocellular carcinoma. *Int J Mol Sci* 2014; **15**: 5762-5773 [PMID: 24714086 DOI: 10.3390/ijms15045762]

4 **Laggai S**, Simon Y, Ranssweiler T, Kiemer AK, Kessler SM. Rapid chromatographic method to decipher distinct alterations in lipid classes in NAFLD/NASH. *World J Hepatol* 2013; **5**: 558-567 [PMID: 24179615 DOI: 10.4254/wjh.v5.i10.558]

5 **Laggai S**, Kessler SM, Boettcher S, Lebrun V, Gemperlein K, Lederer E, Leclercq IA, Mueller R, Hartmann RW, Haybaeck J, Kiemer AK. The IGF2 mRNA binding protein p62/IGF2BP2-2 induces fatty acid elongation as a critical feature of steatosis. *J Lipid Res* 2014; **55**: 1087-1097 [PMID: 24755648 DOI: 10.1194/jlr.M045500]

6 **Muir K**, Hazim A, He Y, Peyressatre M, Kim DY, Song X, Beretta L. Proteomic and lipidomic signatures of lipid metabolism in NASH-associated hepatocellular carcinoma. *Cancer Res* 2013; **73**: 4722-4731 [PMID: 23749645 DOI: 10.1158/0008-5472.CAN-12-3797]

7 **Kessler SM**, Laggai S, Barghash A, Helms V, Kiemer AK. Lipid metabolism signatures in NASH-associated HCC.--letter. *Cancer Res* 2014; **74**: 2903-2904 [PMID: 24778416 DOI: 10.1158/0008-5472.CAN-13-2852.]

8 **Larter CZ**, Yeh MM, Haigh WG, Williams J, Brown S, Bell-Anderson KS, Lee SP, Farrell GC. Hepatic free fatty acids accumulate in experimental steatohepatitis: role of adaptive pathways. *J Hepatol* 2008; **48**: 638-647 [PMID: 18280001 DOI: 10.1016/j.jhep.2007.12.011]

9 **Farrell GC**, van Rooyen D. Liver cholesterol: is it playing possum in NASH? *Am J Physiol Gastrointest Liver Physiol* 2012; **303**: G9-11 [PMID: 22556144 DOI: 10.1152/ajpgi.00008.2012]

10 **Ioannou GN**, Haigh WG, Thorning D, Savard C. Hepatic cholesterol crystals and crown-like structures distinguish NASH from simple steatosis. *J Lipid Res* 2013; **54**: 1326-1334 [PMID: 23417738 DOI: 10.1194/jlr.M034876]

11 **Puri P**, Wiest MM, Cheung O, Mirshahi F, Sargeant C, Min HK, Contos MJ, Sterling RK, Fuchs M, Zhou H, Watkins SM, Sanyal AJ. The plasma lipidomic signature of nonalcoholic steatohepatitis. *Hepatology* 2009; **50**: 1827-1838 [PMID: 19937697 DOI: 10.1158/0008-5472]

12 **Tomita K**, Teratani T, Suzuki T, Shimizu M, Sato H, Narimatsu K, Okada Y, Kurihara C, Irie R, Yokoyama H, Shimamura K, Usui S, Ebinuma H, Saito H, Watanabe C, Komoto S, Kawaguchi A, Nagao S, Sugiyama K, Hokari R, Kanai T, Miura S, Hibi T. Free cholesterol accumulation in hepatic stellate cells: mechanism of liver fibrosis aggravation in nonalcoholic steatohepatitis in mice. *Hepatology* 2014; **59**: 154-169 [PMID: 23832448 DOI: 10.1002/hep.26604]

13 **Wouters K**, van Gorp PJ, Bieghs V, Gijbels MJ, Duimel H, Lütjohann D, Kerksiek A, van Kruchten R, Maeda N, Staels B, van Bilsen M, Shiri-Sverdlov R, Hofker MH. Dietary cholesterol, rather than liver steatosis, leads to hepatic inflammation in hyperlipidemic mouse models of nonalcoholic steatohepatitis. *Hepatology* 2008; **48**: 474-486 [PMID: 18666236 DOI: 10.1002/hep.22363]

14 **Zhang JY**, Chan EK, Peng XX, Tan EM. A novel cytoplasmic protein with RNA-binding motifs is an autoantigen in human hepatocellular carcinoma. *J Exp Med* 1999; **189**: 1101-1110 [PMID: 10190901 DOI: 10.1084/jem.189.7.1101]

15 **Lu M**, Nakamura RM, Dent ED, Zhang JY, Nielsen FC, Christiansen J, Chan EK, Tan EM. Aberrant expression of fetal RNA-binding protein p62 in liver cancer and liver cirrhosis. *Am J Pathol* 2001; **159**: 945-953 [PMID: 11549587 DOI: 10.1016/S0002-9440(10)61770-1]

16 **Kessler SM**, Pokorny J, Zimmer V, Laggai S, Lammert F, Bohle RM, Kiemer AK. IGF2 mRNA binding protein p62/IMP2-2 in hepatocellular carcinoma: antiapoptotic action is independent of IGF2/PI3K signaling. *Am J Physiol Gastrointest Liver Physiol* 2013; **304**: G328-G336 [PMID: 23257922 DOI: 10.1152/ajpgi.00005.2012]

17 **Bell JL**, Wächter K, Mühleck B, Pazaitis N, Köhn M, Lederer M, Hüttelmaier S. Insulin-like growth factor 2 mRNA-binding proteins (IGF2BPs): post-transcriptional drivers of cancer progression? *Cell Mol Life Sci* 2013; **70**: 2657-2675 [PMID: 23069990 DOI: 10.1007/s00018-012-1186-z]

18 **Simon Y**, Kessler SM, Bohle RM, Haybaeck J, Kiemer AK. The insulin-like growth factor 2 (IGF2) mRNA-binding protein p62/IGF2BP2-2 as a promoter of NAFLD and HCC? *Gut* 2014; **63**: 861-863 [PMID: 24173291 DOI: 10.1136/gutjnl-2013-305736]

19 **Tybl E**, Shi FD, Kessler SM, Tierling S, Walter J, Bohle RM, Wieland S, Zhang J, Tan EM, Kiemer AK. Overexpression of the IGF2-mRNA binding protein p62 in transgenic mice induces a steatotic phenotype. *J Hepatol* 2011; **54**: 994-1001 [PMID: 21145819 DOI: 10.1016/j.jhep.2010.08.034]

20 **Liu Y**, Meyer C, Xu C, Weng H, Hellerbrand C, ten Dijke P, Dooley S. Animal models of chronic liver diseases. *Am J Physiol Gastrointest Liver Physiol* 2013; **304**: G449-G468 [PMID: 23275613 DOI: 10.1152/ajpgi.00199.2012]

21 **Corradini E**, Pietrangelo A. Iron and steatohepatitis. *J Gastroenterol Hepatol* 2012; **27** Suppl 2: 42-46 [PMID: 22320915 DOI: 10.1111/j.1440-1746.2011.07014.x]

22 **Bouayed J**, Desor F, Rammal H, Kiemer AK, Tybl E, Schroeder H, Rychen G, Soulimani R. Effects of lactational exposure to benzo[alpha]pyrene (B[alpha]P) on postnatal neurodevelopment, neuronal receptor gene expression and behaviour in mice. *Toxicology* 2009; **259**: 97-106 [PMID: 19428949 DOI: 10.1016/j.tox.2009.02.010]

23 **Garcia R**, Pistorius D, Stadler M, Müller R. Fatty acid-related phylogeny of myxobacteria as an approach to discover polyunsaturated omega-3/6 Fatty acids. *J Bacteriol* 2011; **193**: 1930-1942 [PMID: 21317327 DOI: 10.1128/JB.01091-10]

24 **Koerber K**, Sass G, Kiemer AK, Vollmar AM, Tiegs G. In vivo regulation of inducible no synthase in immune-mediated liver injury in mice. *Hepatology* 2002; **36**: 1061-1069 [PMID: 12395315 DOI: 10.1053/jhep.2002.36155]

25 **Yao ZM**, Vance DE. The active synthesis of phosphatidylcholine is required for very low density lipoprotein secretion from rat hepatocytes. *J Biol Chem* 1988; **263**: 2998-3004 [PMID: 3343237]

26 **Yamazaki Y**, Kakizaki S, Takizawa D, Ichikawa T, Sato K, Takagi H, Mori M. Interstrain differences in susceptibility to non-alcoholic steatohepatitis. *J Gastroenterol Hepatol* 2008; **23**: 276-282 [PMID: 17868334 DOI: 10.1111/j.1440-1746.2007.05150.x]

27 **Graham RM**, Chua AC, Carter KW, Delima RD, Johnstone D, Herbison CE, Firth MJ, O'Leary R, Milward EA, Olynyk JK, Trinder D. Hepatic iron loading in mice increases cholesterol biosynthesis. *Hepatology* 2010; **52**: 462-471 [PMID: 20683946 DOI: 10.1002/hep.23712]

28 **Caballero F**, Fernández A, De Lacy AM, Fernández-Checa JC, Caballería J, García-Ruiz C. Enhanced free cholesterol, SREBP-2 and StAR expression in human NASH. *J Hepatol* 2009; **50**: 789-796 [PMID: 19231010 DOI: 10.1016/j.jhep.2008.12.016]

29 **Min HK**, Kapoor A, Fuchs M, Mirshahi F, Zhou H, Maher J, Kellum J, Warnick R, Contos MJ, Sanyal AJ. Increased hepatic synthesis and dysregulation of cholesterol metabolism is associated with the severity of nonalcoholic fatty liver disease. *Cell Metab* 2012; **15**: 665-674 [PMID: 22560219 DOI: 10.1016/j.cmet.2012.04.004]

30 **Smits MM**, Ioannou GN, Boyko EJ, Utzschneider KM. Non-alcoholic fatty liver disease as an independent manifestation of the metabolic syndrome: results of a US national survey in three ethnic groups. *J Gastroenterol Hepatol* 2013; **28**: 664-670 [PMID: 23286209 DOI: 10.1111/jgh.12106]

31 **Glosli H**, Gudbrandsen OA, Mullen AJ, Halvorsen B, Røst TH, Wergedahl H, Prydz H, Aukrust P, Berge RK. Down-regulated expression of PPARalpha target genes, reduced fatty acid oxidation and altered fatty acid composition in the liver of mice transgenic for hTNFalpha. *Biochim Biophys Acta* 2005; **1734**: 235-246 [PMID: 15893958 DOI: 10.1016/j.bbalip.2005.02.011]

32 **Abiru S**, Migita K, Maeda Y, Daikoku M, Ito M, Ohata K, Nagaoka S, Matsumoto T, Takii Y, Kusumoto K, Nakamura M, Komori A, Yano K, Yatsuhashi H, Eguchi K, Ishibashi H. Serum cytokine and soluble cytokine receptor levels in patients with non-alcoholic steatohepatitis. *Liver Int* 2006; **26**: 39-45 [PMID: 16420507 DOI: 10.1111/j.1478-3231.2005.01191.x]

33 **Feldstein AE**, Canbay A, Angulo P, Taniai M, Burgart LJ, Lindor KD, Gores GJ. Hepatocyte apoptosis and fas expression are prominent features of human nonalcoholic steatohepatitis. *Gastroenterology* 2003; **125**: 437-443 [PMID: 12891546 DOI: 10.1016/S0016-5085(03)00907-7]

34 **Albano E**, Mottaran E, Vidali M, Reale E, Saksena S, Occhino G, Burt AD, Day CP. Immune response towards lipid peroxidation products as a predictor of progression of non-alcoholic fatty liver disease to advanced fibrosis. *Gut* 2005; **54**: 987-993 [PMID: 15951547 DOI: 10.1136/gut.2004.057968]

35 **Yu J**, Ip E, Dela Peña A, Hou JY, Sesha J, Pera N, Hall P, Kirsch R, Leclercq I, Farrell GC. COX-2 induction in mice with experimental nutritional steatohepatitis: Role as pro-inflammatory mediator. *Hepatology* 2006; **43**: 826-836 [PMID: 16557554 DOI: 10.1002/hep.21108]

36 **Stienstra R**, Saudale F, Duval C, Keshtkar S, Groener JE, van Rooijen N, Staels B, Kersten S, Müller M. Kupffer cells promote hepatic steatosis via interleukin-1beta-dependent suppression of peroxisome proliferator-activated receptor alpha activity. *Hepatology* 2010; **51**: 511-522 [PMID: 20054868 DOI: 10.1002/hep.23337]

37 **Paillard F**, Catheline D, Duff FL, Bouriel M, Deugnier Y, Pouchard M, Daubert JC, Legrand P. Plasma palmitoleic acid, a product of stearoyl-coA desaturase activity, is an independent marker of triglyceridemia and abdominal adiposity. *Nutr Metab Cardiovasc Dis* 2008; **18**: 436-440 [PMID: 18068341 DOI: 10.1016/j.numecd.2007.02.017]

38 **Miyazaki M**, Bruggink SM, Ntambi JM. Identification of mouse palmitoyl-coenzyme A Delta9-desaturase. *J Lipid Res* 2006; **47**: 700-704 [PMID: 16443825 DOI: 10.1194/jlr.C500025-JLR200]

39 **Ntambi JM**, Miyazaki M. Regulation of stearoyl-CoA desaturases and role in metabolism. *Prog Lipid Res* 2004; **43**: 91-104 [PMID: 14654089 DOI: 10.1016/S0163-7827(03)00039-0]

40 **Matsuzaka T**, Atsumi A, Matsumori R, Nie T, Shinozaki H, Suzuki-Kemuriyama N, Kuba M, Nakagawa Y, Ishii K, Shimada M, Kobayashi K, Yatoh S, Takahashi A, Takekoshi K, Sone H, Yahagi N, Suzuki H, Murata S, Nakamuta M, Yamada N, Shimano H. Elovl6 promotes nonalcoholic steatohepatitis. *Hepatology* 2012; **56**: 2199-2208 [PMID: 22753171 DOI: 10.1002/hep.25932]

41 **Anstee QM**, Goldin RD. Mouse models in non-alcoholic fatty liver disease and steatohepatitis research. *Int J Exp Pathol* 2006; **87**: 1-16 [PMID: 16436109 DOI: 10.1111/j.0959-9673.2006.00465.x]

42 **Musso G**, Gambino R, Cassader M. Cholesterol metabolism and the pathogenesis of non-alcoholic steatohepatitis. *Prog Lipid Res* 2013; **52**: 175-191 [PMID: 23206728 DOI: 10.1016/j.plipres.2012.11.002]

43 **Farrell GC**, van Rooyen D, Gan L, Chitturi S. NASH is an Inflammatory Disorder: Pathogenic, Prognostic and Therapeutic Implications. *Gut Liver* 2012; **6**: 149-171 [PMID: 22570745 DOI: 10.5009/gnl.2012.6.2.149]

44 **Fujita N**, Miyachi H, Tanaka H, Takeo M, Nakagawa N, Kobayashi Y, Iwasa M, Watanabe S, Takei Y. Iron overload is associated with hepatic oxidative damage to DNA in nonalcoholic steatohepatitis. *Cancer Epidemiol Biomarkers Prev* 2009; **18**: 424-432 [PMID: 19190144 DOI: 10.1158/1055-9965.EPI-08-0725]

45 **Sorrentino P**, D'Angelo S, Ferbo U, Micheli P, Bracigliano A, Vecchione R. Liver iron excess in patients with hepatocellular carcinoma developed on non-alcoholic steato-hepatitis. *J Hepatol* 2009; **50**: 351-357 [PMID: 19070395 DOI: 10.1016/j.jhep.2008.09.011]

46 **Ahmed U**, Latham PS, Oates PS. Interactions between hepatic iron and lipid metabolism with possible relevance to steatohepatitis. *World J Gastroenterol* 2012; **18**: 4651-4658 [PMID: 23002334 DOI: 10.3748/wjg.v18.i34.4651]

47 **Pigeon C**, Legrand P, Leroyer P, Bouriel M, Turlin B, Brissot P, Loréal O. Stearoyl coenzyme A desaturase 1 expression and activity are increased in the liver during iron overload. *Biochim Biophys Acta* 2001; **1535**: 275-284 [PMID: 11278167 DOI: 10.1016/S0925-4439(01)00024-2]

48 **Philippe MA**, Ruddell RG, Ramm GA. Role of iron in hepatic fibrosis: one piece in the puzzle. *World J Gastroenterol* 2007; **13**: 4746-4754 [PMID: 17729396]

49 **Seki S**, Kitada T, Yamada T, Sakaguchi H, Nakatani K, Wakasa K. In situ detection of lipid peroxidation and oxidative DNA damage in non-alcoholic fatty liver diseases. *J Hepatol* 2002; **37**: 56-62 [PMID: 12076862 DOI: 10.1016/S0168-8278(02)00073-9]

P- Reviewer: Vespasiani-Gentilucci U **S- Editor**: Ding Y
L- Editor: AmEditor **E- Editor**: Zhang DN

Published by **Baishideng Publishing Group Inc**
8226 Regency Drive, Pleasanton, CA 94588, USA
Telephone: +1-925-223-8242
Fax: +1-925-223-8243
E-mail: bpgoffice@wjgnet.com
Help Desk: http://www.wjgnet.com/esps/helpdesk.aspx
http://www.wjgnet.com

ISSN 1007-9327